Organo–Platinum–Iron Complexes containing One Bridging $Ph_2PCH_2PPh_2$ Ligand. Crystal Structures of $[(OC)_3Fe(\mu\text{-dppm})(\mu\text{-CO})Pt(PPh_3)]$, $[(OC)_2Fe(\mu\text{-dppm})\{\mu\text{-C(O)}C_2H_2\}Pt(PPh_3)]$, and $[(OC)_3Fe(\mu\text{-dppm})(\mu\text{-CMe=CH}_2)Pt(PPh_3)][BF_4]$ †

Xavier L. R. Fontaine, Grant B. Jacobsen, Bernard L. Shaw,* and Mark Thornton-Pett
School of Chemistry, University of Leeds, Leeds LS2 9JT

Treatment of $[Fe(CO)_4(dppm\text{-}P)]$ (dppm = $Ph_2PCH_2PPh_2$) with $[Pt(trans\text{-}PhCH{=}CHPh)(PPh_3)_2]$ gave the bimetallic $[(OC)_3Fe(\mu\text{-dppm})(\mu\text{-CO})Pt(PPh_3)]$ (**1**) in 75% isolated yield. Complex (**1**) was also prepared by the sodium tetrahydroborate reduction of $[(OC)_3Fe(\mu\text{-dppm})(\mu\text{-CO})PtCl_2]$ in the presence of PPh_3. Its structure was established by *X*-ray crystallography: the crystals are triclinic, space group $P\bar{1}$, with a = 1 177.3(2), b = 1 198.4(1), c = 1 776.5(1) pm, α = 103.34(1), β = 107.81(1), γ = 91.76(1)°, and Z = 2; final R factor 0.0257 for 5 422 observed reflections. The structure shows that one of the carbonyl ligands is almost symmetrically bridging the Fe–Pt bond. Protonation of complex (**1**) with $HBF_4{\cdot}OEt_2$ gave the hydride $[(OC)_4Fe(\mu\text{-dppm})PtH(PPh_3)][BF_4]$ (**4**), ^1H n.m.r. studies of which indicated the hydride ligand to be terminal on platinum. Ethyne reacted with (**1**) at 20 °C to give the complex $[(OC)_2Fe(\mu\text{-dppm})\{\mu\text{-C(O)}C_2H_2\}Pt(PPh_3)]$ (**5**), the structure of which was established by *X*-ray crystallography: the crystals are orthorhombic, space group *Pbca*, with a = 1 898.9(4), b = 1 828.3(3), c = 2 414.4(5) pm, and Z = 8; R 0.0381 for 4 163 observed reflections. The molecule contains a dimetallacyclopentenone ring in which the ethylenic bond is η^2-bound to iron, so that the $C(O)C_2H_2$ moiety is σ-co-ordinated to platinum and η^3-co-ordinated to iron. Unsymmetrical alkynes (MeC≡CH, PhC≡CH, 4-MeC_6H_4C≡CH, $MeNHCH_2$C≡CH, $HOMe_2$CC≡CH, and $MeCO_2$C≡CH) also reacted with complex (**1**), at 80 °C, to give complexes of type $[(OC)_2Fe(\mu\text{-dppm})\{\mu\text{-C(O)CRCH}\}Pt(PPh_3)]$. At 20 °C, MeC≡CH and 4-MeC_6H_4C≡CH reacted with (**1**) to give isolable complexes of type $[(OC)_2Fe(\mu\text{-dppm})\{\mu\text{-C(O)CHCR}\}Pt(PPh_3)]$ which isomerised in solution, at rates dependent on the steric bulk of R, to complexes of type $[(OC)_2Fe(\mu\text{-dppm})\{\mu\text{-C(O)CRCH}\}Pt(PPh_3)]$. The mechanism of the alkyne-insertion reactions appears to involve an intermediate containing a monodentate dppm ligand co-ordinated to iron, formed by opening of the five-membered FePCPPt ring in (**1**). Protonation of the alkyne complexes breaks the alkyne–CO link to give μ-vinyl cations of type $[(OC)_3Fe(\mu\text{-dppm})(\mu\text{-CR=CH}_2)Pt(PPh_3)]^+$ (R = H, Me, or C_6H_4Me-4). The structure of $[(OC)_3Fe(\mu\text{-dppm})(\mu\text{-CMe=CH}_2)Pt(PPh_3)][BF_4]$ (**16**) has also been established by *X*-ray crystallography: the crystals are monoclinic, space group *Cc*, with a = 2 321.3(3), b = 1 091.2(2), c = 1 962.6(2) pm, β = 98.48(1)°, and Z = 4, R 0.0460 for 3 615 observed reflections. The structure shows that the μ-CMe=CH_2 moiety is σ-co-ordinated to platinum and η^2-co-ordinated to iron. Treatment of complex (**1**) with $MeO_2CC{\equiv}CCO_2Me$ displaced the PPh_3 ligand to give $[(OC)_4Fe(\mu\text{-dppm})Pt(MeO_2CC{\equiv}CCO_2Me)]$ (**19**). The complex $[(OC)_3Fe(\mu\text{-dppm})(\mu\text{-SO}_2)Pt(PPh_3)]$ (**20**) was formed in high yield when SO_2 was bubbled through a dichloromethane solution of (**1**). In addition, analogues of many of the above complexes have been prepared with $(Ph_2P)_2C{=}CH_2$.

In recent publications we have reported the use of the monodentate diphosphine–iron complex $[Fe(CO)_4(dppm\text{-}P)]$ (dppm = $Ph_2PCH_2PPh_2$) in the systematic synthesis of heterobimetallic complexes with Mn^I, Mo^0,[1] Rh^I,[2] Pt^{II},[3,4] or Pd^{II}.[3,4]

The complexes $[Fe(CO)_5]$ and $[Fe(CO)_4(PR_3)]$ are inert towards substitution by olefins or acetylenes; $[Fe(CO)_4(dppm\text{-}P)]$ is similarly inert, *e.g.* we have recovered it unchanged after heating it with an excess of PhC≡CH in benzene solution at 80 °C for 2 h. We reasoned that, if we could attach the $[Fe(CO)_4(dppm\text{-}P)]$ to a centre which was labile towards substitution by olefins or acetylenes, the iron centre might then react with the organic substrate by an intramolecular process. A platinum(0) centre of the type $Pt(PR_3)_2$ seemed suitable since complexes of the types $[Pt(olefin)(PR_3)_2]$ or $[Pt(acetylene)(PR_3)_2]$ are labile but stable.

In this paper we describe the synthesis of heterobimetallic complexes of iron(0) carbonyl with platinum(0) and the development of a substantial organic chemistry at the iron–platinum centres. Aspects of this work have appeared as a preliminary communication.[5]

Results and Discussion

Treatment of the monodentate dppm–iron complex $[Fe(CO)_4(dppm\text{-}P)]$[6] with 1 mol equivalent of $[Pt(trans\text{-}PhCH{=}CHPh)(PPh_3)_2]$ in benzene gave the iron–platinum complex $[(OC)_3$-

† μ-Bis(diphenylphosphino)methane-μ-carbonyl-2,2,2-tricarbonyl-1-triphenylphosphineplatinumiron (*Pt–Fe*), μ-bis(diphenylphosphino)-methane-2,2-dicarbonyl-μ-[1-oxoprop-2-ene-1,3-diyl-C^{1-3}(Fe), C^3(Pt)]-1-triphenylphosphineplatinumiron (*Pt–Fe*), and μ-bis(diphenylphosphino)methane-2,2,2-tricarbonyl-μ-[isopropenyl-C^1-(Fe,Pt)-C^2(Fe)]-1-triphenylphosphineplatinumiron (*Pt–Fe*) tetrafluoroborate.

Supplementary data available: see Instructions for Authors, *J. Chem. Soc., Dalton Trans.*, 1988, Issue 1, pp. xvii—xx.

Fe(μ-dppm)(μ-CO)Pt(PPh_3)] (**1**) in 75% isolated yield. The vdpp [$(Ph_2P)_2C{=}CH_2$] analogue [$(OC)_3Fe$(μ-vdpp)(μ-CO)-$Pt(PPh_3)$] (**2**) was similarly prepared from [$Fe(CO)_4$(vdpp-*P*)] in 79% yield. Alternatively, (**1**) was prepared, in 75% yield, by the sodium tetrahydroborate reduction of the iron(0)–platinum(II) complex [$(OC)_3Fe$(μ-dppm)(μ-CO)$PtCl_2$][3,4] in the presence of triphenylphosphine in dichloromethane. In this way, the tri-*p*-tolylphosphine analogue [$(OC)_3Fe$(μ-dppm)-(μ-CO)Pt{$P(C_6H_4Me$-4)$_3$}] (**3**) was also prepared. The complexes (**1**)—(**3**) were characterised by elemental analysis and i.r. (Table 1), ^{31}P-{^1H} (Table 2), and ^1H (Table 3) n.m.r. spectroscopy; preparative details are given in the Experimental section. In addition, the structure of (**1**) has been determined by *X*-ray crystallography (see below). The ^{31}P-{^1H} n.m.r. spectra of complexes (**1**)—(**3**) were similar [Figure 1 illustrates the spectrum of (**1**)], each consisting of three resonances: a low-field resonance with satellites due to a small coupling to ^{195}Pt (*J* 49—81 Hz) assigned to the phosphorus atom bonded to iron and two higher-field resonances, also with ^{195}Pt satellites (*J ca.* 4 500 and *ca.* 2 500 Hz) assigned to the phosphorus atoms bonded to platinum. The large value of $^2J(P_AP_B)$ of *ca.* 185 Hz within the dppm or vdpp ligands made possible the individual assignments of each of the phosphorus atoms on platinum, *i.e.* P_B and P_C.

A two-dimensional COSY ^{31}P-{^1H} n.m.r. spectrum of complex (**1**) established that $J(PtP_A)$ was 66, $J(PtP_B)$ = +2 509, and $J(PtP_C)$ = +4 566 Hz (one-bond Pt–P couplings are always positive).

The i.r. spectra of complexes (**1**)—(**3**) were similar in the carbonyl region, showing bands assigned to terminal carbonyl ligands and a low-energy band at *ca.* 1 760 cm^{-1} indicating a bridging carbonyl.

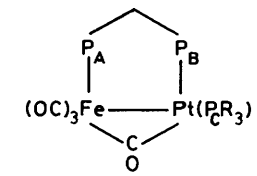

	P P	R
(1)	dppm	Ph
(2)	vdpp	Ph
(3)	dppm	C_6H_4Me-4

Table 1. Infrared[a] and analytical data[b]

Complex	ν(C≡O)/cm^{-1}	Analyses (%) C	H
(**1**)·1.5C_6H_6	2 005s, 1 932m, 1 760m	57.65 (57.9)	3.85 (4.3)
(**2**)	2 002s, 1 934m, 1 758m	56.45 (56.45)	3.7 (3.65)
(**3**)	2 000s, 1 928s, 1 756m	56.85 (57.1)	4.2 (4.1)
(**4**)	2 078s, 2 024m, 1 988m, 1 948m	50.55 (51.45)	3.6 (3.5)
(**5**)	1 968s, 1 916s, 1 690m	57.15 (56.8)	3.85 (3.8)
(**6a**)	1 960s, 1 910s, 1 688m	57.7 (57.6)	4.25 (4.05)
(**6b**)	1 960s, 1 908s, 1 680m	57.55 (57.6)	4.3 (4.05)
(**7a**)	1 965s, 1 915s, 1 687m	60.15 (59.75)	4.05 (4.05)
(**7b**)	1 965s, 1 916s, 1 692m	59.8 (59.25)	4.15 (4.05)
(**8**)	1 968s, 1 916s, 1 680m	60.1 (60.15)	4.15 (4.0)
(**9**)	1 965s, 1 912s, 1 685m	60.15 (59.4)	4.25 (3.9)
(**10**)[c]	1 960s, 1 910s, 1 692m	56.75 (56.8)	4.4 (4.1)
(**11**)[d]	1 960s, 1 910s, 1 690m	57.25 (57.3)	4.3 (4.0)
(**12**)	1 960s, 1 908s, 1 672m	56.9 (57.1)	4.3 (4.15)
(**13**)·0.5C_6H_{14}	1 964s, 1 912s, 1 690m	59.1 (58.6)	4.25 (4.55)
(**14**)	1 976s, 1 926s, 1 694m	—	—
(**15**)·CH_2Cl_2	2 048s, 1 996s, 1 968s	50.2 (49.85)	3.9 (3.6)
(**16**)·0.5CH_2Cl_2	2 040s, 1 992s, 1 964s	51.3 (51.6)	3.9 (3.75)
(**17**)	2 046s, 2 005s, 1 927m	—	—
(**18**)	2 040s, 1 998s, 1 914m	55.6 (56.25)	3.95 (3.85)
(**19**)	2 062s, 2 018s, 1 964s, 1 944s, 1 695s	47.6 (47.25)	3.25 (3.15)
(**20**)[e]	2 034s, 1 972s	52.2 (52.6)	3.8 (3.45)

[a] As solutions in dichloromethane; s = strong and m = medium. [b] Calculated values in parentheses. [c] N 1.65 (1.3%). [d] N 1.5 (1.3%). [e] S 3.55 (3.0%).

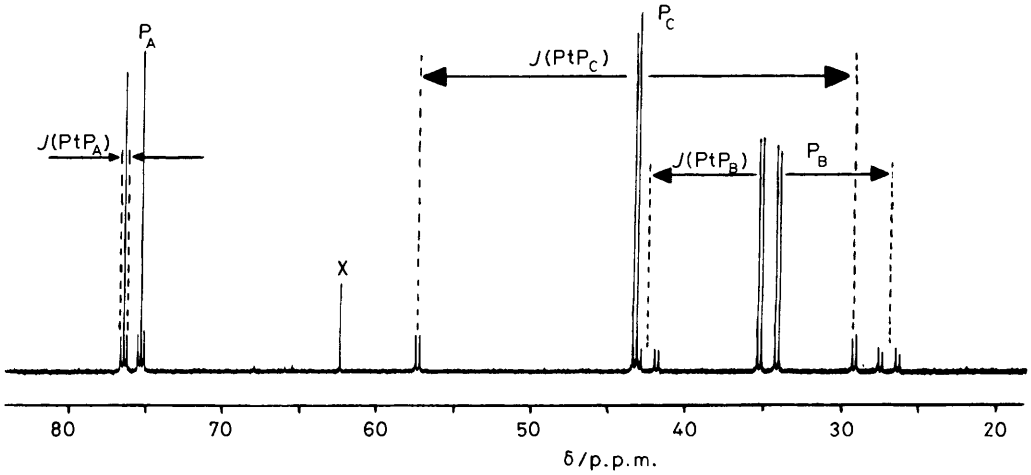

Figure 1. 162-MHz ^{31}P-{^1H} N.m.r. spectrum of [$(OC)_3Fe$(μ-dppm)(μ-CO)$Pt(PPh_3)$] (**1**) in CD_2Cl_2 at 20 °C. X = Impurity

Table 2. ^{31}P-{^{1}H} N.m.r. data*

Complex		Complex	
(1)	75.9 [d, P_A, $J(P_AP_B)$ 182, $J(PtP_A)$ 66] 43.3 [d, P_C, $J(P_BP_C)$ 41, $J(PtP_C)$ 4 566] 34.7 [dd, P_B, $J(P_AP_B)$ 182, $J(P_BP_C)$ 41, $J(PtP_B)$ 2 509]	**(10)**	59.7 [dd, P_A, $J(P_AP_B)$ 56, $J(P_AP_C)$ 34, $J(PtP_A)$ 142] 33.2 [dd, P_C, $J(P_AP_C)$ 34, $J(P_BP_C)$ 5, $J(PtP_C)$ 3 415] 7.9 [dd, P_B, $J(P_AP_B)$ 56, $J(P_BP_C)$ 5, $J(PtP_B)$ 2 636]
(2)	66.5 [dd, P_A, $J(P_AP_B)$ 192, $J(P_AP_C)$ 17, $J(PtP_A)$ 81] 43.4 [dd, P_C, $J(P_AP_C)$ 17, $J(P_BP_C)$ 47, $J(PtP_C)$ 4 596] 27.5 [dd, P_B, $J(P_AP_B)$ 192, $J(P_BP_C)$ 47, $J(PtP_B)$ 2 714]	**(11)**	75.1 [dd, P_A, $J(P_AP_B)$ 115, $J(P_AP_C)$ 31, $J(PtP_A)$ 128] 30.9 [dd, P_C, $J(P_AP_C)$ 31, $J(P_BP_C)$ 3, $J(PtP_C)$ 3 435] 27.2 [dd, P_B, $J(P_AP_B)$ 115, $J(P_BP_C)$ 3, $J(PtP_B)$ 2 746]
(3)	76.9 [d, P_A, $J(P_AP_B)$ 181, $J(PtP_A)$ 49] 42.1 [d, P_C, $J(P_BP_C)$ 39, $J(PtP_C)$ 4 582] 35.0 [dd, P_B, $J(P_AP_B)$ 181, $J(P_BP_C)$ 39, $J(PtP_B)$ 2 478]	**(12)**	58.5 [dd, P_A, $J(P_AP_B)$ 59, $J(P_AP_C)$ 36, $J(PtP_A)$ 140] 32.8 [dd, P_C, $J(P_AP_C)$ 36, $J(P_BP_C)$ 5, $J(PtP_C)$ 3 523] 6.7 [dd, P_B, $J(P_AP_B)$ 59, $J(P_BP_C)$ 5, $J(PtP_B)$ 2 651]
(4)	70.3 [dd, P_A, $J(P_AP_B)$ 86, $J(P_AP_C)$ 12, $J(PtP_A)$ 80] 29.5 [br d, P_B, $J(P_AP_B)$ 86, $J(PtP_B)$ 2 150] 26.6 [dd, P_C, $J(P_AP_C)$ 12, $J(P_BP_C)$ 11, $J(PtP_C)$ 3 850]	**(13)**	76.0 [dd, P_A, $J(P_AP_B)$ 112, $J(P_AP_C)$ 31, $J(PtP_A)$ 114] 31.3 [dd, P_C, $J(P_AP_C)$ 31, $J(P_BP_C)$ 3, $J(PtP_C)$ 3 486] 26.8 [dd, P_B, $J(P_AP_B)$ 112, $J(P_BP_C)$ 3, $J(PtP_B)$ 2 750]
(5)	59.6 [dd, P_A, $J(P_AP_B)$ 59, $J(P_AP_C)$ 37, $J(PtP_A)$ 140] 32.9 [dd, P_C, $J(P_AP_C)$ 37, $J(P_BP_C)$ 6, $J(PtP_C)$ 3 365] 7.6 [dd, P_B, $J(P_AP_B)$ 59, $J(P_BP_C)$ 6, $J(PtP_B)$ 2 605]	**(14)**	60.9 [dd, P_A, $J(P_AP_B)$ 51, $J(P_AP_C)$ 32, $J(PtP_A)$ 112] 33.5 [dd, P_C, $J(P_AP_C)$ 32, $J(P_BP_C)$ 10, $J(PtP_C)$ 3 456] 5.6 [dd, P_B, $J(P_AP_B)$ 51, $J(P_BP_C)$ 10, $J(PtP_B)$ 2 688]
(6a)	60.4 [dd, P_A, $J(P_AP_B)$ 61, $J(P_AP_C)$ 34, $J(PtP_A)$ 142] 33.0 [dd, P_C, $J(P_AP_C)$ 34, $J(P_BP_C)$ 7, $J(PtP_C)$ 3 359] 7.4 [dd, P_B, $J(P_AP_B)$ 61, $J(P_BP_C)$ 7, $J(PtP_B)$ 2 500]	**(15)**	52.7 [dd, P_A, $J(P_AP_B)$ 42, $J(P_AP_C)$ 23, $J(PtP_A)$ 64] 33.8 [dd, P_C, $J(P_AP_C)$ 23, $J(P_BP_C)$ 17, $J(PtP_C)$ 3 733] 8.0 [dd, P_B, $J(P_AP_B)$ 42, $J(P_BP_C)$ 17, $J(PtP_B)$ 2 383]
(6b)	60.3 [dd, P_A, $J(P_AP_B)$ 58, $J(P_AP_C)$ 37, $J(PtP_A)$ 135] 33.5 [dd, P_C, $J(P_AP_C)$ 37, $J(P_BP_C)$ 4, $J(PtP_C)$ 3 414] 7.6 [dd, P_B, $J(P_AP_B)$ 58, $J(P_BP_C)$ 4, $J(PtP_B)$ 2 652]	**(16)**	55.6 [dd, P_A, $J(P_AP_B)$ 47, $J(P_AP_C)$ 23, $J(PtP_A)$ 62] 33.7 [dd, P_C, $J(P_AP_C)$ 23, $J(P_BP_C)$ 15, $J(PtP_C)$ 3 760] 8.3 [dd, P_B, $J(P_AP_B)$ 47, $J(P_BP_C)$ 15, $J(PtP_B)$ 2 310]
(7a)	62.6 [dd, P_A, $J(P_AP_B)$ 59, $J(P_AP_C)$ 34, $J(PtP_A)$ 130] 34.8 [dd, P_C, $J(P_AP_C)$ 34, $J(P_BP_C)$ 7, $J(PtP_C)$ 3 336] 8.9 [dd, P_B, $J(P_AP_B)$ 59, $J(P_BP_C)$ 7, $J(PtP_B)$ 2 560]	**(17)**	51.0 [dd, P_A, $J(P_AP_B)$ 50, $J(P_AP_C)$ 27, $J(PtP_A)$ 58] 34.3 [dd, P_C, $J(P_AP_C)$ 27, $J(P_BP_C)$ 17, $J(PtP_C)$ 3 756] 4.85 [dd, P_B, $J(P_AP_B)$ 50, $J(P_BP_C)$ 17, $J(PtP_B)$ 2 250]
(7b)	60.1 [dd, P_A, $J(P_AP_B)$ 60, $J(P_AP_C)$ 37, $J(PtP_A)$ 139] 33.6 [dd, P_C, $J(P_AP_C)$ 37, $J(P_BP_C)$ 4, $J(PtP_C)$ 3 440] 8.0 [br d, P_B, $J(P_AP_B)$ 60, $J(PtP_B)$ 2 680]	**(18)**	62.5 [dd, P_A, $J(P_AP_B)$ 104, $J(P_AP_C)$ 23, $J(PtP_A)$ 66] 33.9 [dd, P_C, $J(P_AP_C)$ 23, $J(P_BP_C)$ 15, $J(PtP_C)$ 3 768] 20.1 [dd, P_B, $J(P_AP_B)$ 104, $J(P_BP_C)$ 15, $J(PtP_B)$ 2 322]
(8)	75.4 [dd, P_A, $J(P_AP_B)$ 115, $J(P_AP_C)$ 31, $J(PtP_A)$ 127] 31.6 [d, P_C, $J(P_AP_C)$ 31, $J(PtP_C)$ 3 471] 27.2 [d, P_B, $J(P_AP_B)$ 115, $J(PtP_B)$ 2 762]	**(19)**	74.5 [d, P_A, $J(P_AP_B)$ 125, $J(PtP_A)$ 126] 24.2 [d, P_B, $J(P_AP_B)$ 125, $J(PtP_B)$ 1 990]
(9)	59.4 [dd, P_A, $J(P_AP_B)$ 56, $J(P_AP_C)$ 36, $J(PtP_A)$ 132] 33.4 [dd, P_C, $J(P_AP_C)$ 36, $J(P_BP_C)$ 5, $J(PtP_C)$ 3 567] 7.5 [dd, P_B, $J(P_AP_B)$ 56, $J(P_BP_C)$ 5, $J(PtP_C)$ 2 712]	**(20)**	70.6 [dd, P_A, $J(P_AP_B)$ 136, $J(P_AP_C)$ 5, $J(PtP_A)$ 71] 30.2 [dd, P_C, $J(P_AP_C)$ 5, $J(P_BP_C)$ 12, $J(PtP_C)$ 4 142] 25.2 [dd, P_B, $J(P_AP_B)$ 136, $J(P_BP_C)$ 12, $J(PtP_B)$ 2 876]

* Recorded at 162 MHz in CH_2Cl_2 solution and 20 °C. Positive shifts to high frequency of external 85% H_3PO_4. Coupling constants in Hz. P_A and P_B refer to the dppm or vdpp phosphorus atoms bonded to iron and platinum, respectively, P_C to the triphenylphosphine phosphorus atom. The multiplicity *e.g.* d or dd refers to the P–P coupling.

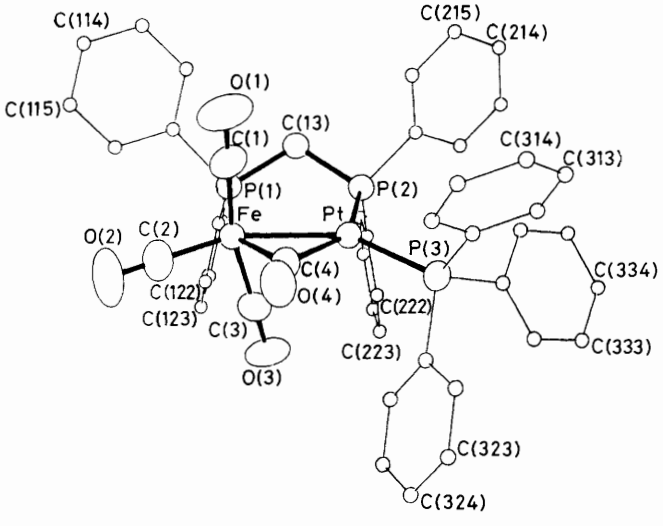

Figure 2. Molecular structure of $[(OC)_3Fe(\mu\text{-dppm})(\mu\text{-CO})Pt(PPh_3)]$ (**1**) showing the principal atomic numbering

Crystal Structure of $[(OC)_3Fe(\mu\text{-dppm})(\mu\text{-CO})Pt(PPh_3)]$ (**1**).—Complex (**1**) was crystallised from benzene solution. The structure is shown in Figure 2 and selected intramolecular distances and angles are given in Table 4. The iron and platinum moieties are linked by a single dppm bridge to give a five-membered FePCPPt ring. The Fe–Pt distance of 257.9(4) pm indicates a metal–metal bond and is close to those found in other crystallographically characterised compounds of these metals, *viz.* $[Fe_2Pt(CO)_8(cod)]$ (cod = cyclo-octa-1,5-diene), Fe–Pt 256.1 and 255.3 pm,[7] and $[Fe_2Pt(CO)_9(PPh_3)]$, 260.5 and 252.6 pm.[8] The Pt–C(4) distance, 199.2(7) pm, and Fe–C(4) distance, 201.2(7) pm, suggest that the bridging carbonyl is slightly more strongly bonded to Pt, a feature that is supported by the relative size of the angles, Pt–C(4)–O(4) > Fe–C(4)–O(4). The crystal structure of the related homobimetallic $[(OC)_3Fe(\mu\text{-dppm})(\mu\text{-CO})Fe(CO)_3]$[9] also shows the presence of a symmetrically bridging carbonyl ligand.

Treatment of a dichloromethane solution of complex (**1**) with an excess of $HBF_4{\cdot}OEt_2$ gave the hydride $[(OC)_4Fe(\mu\text{-dppm})PtH(PPh_3)][BF_4]$ (**4**) in 90% yield. It was characterised by elemental analysis, i.r., ^{31}P-{^{1}H}, and ^{1}H n.m.r. spectroscopy (data are in the Tables). The ^{31}P-{^{1}H} n.m.r. spectrum was similar to that of complex (**1**), indicating that the dimetal–phosphine backbone was unchanged. The i.r. spectrum showed four terminal carbonyl bands, suggesting the absence of a bridging carbonyl. In the ^{1}H n.m.r. spectrum, the hydride resonance occurred at −5.53 p.p.m. and selective ^{1}H-{^{31}P} decoupling experiments showed that the hydride was strongly coupled to P_B [$J(P_BH)$ = 179 Hz] clearly in a *trans* position. The n.m.r. parameters of (**4**) are similar to those of the related complex $[(\eta^5\text{-}C_5H_5)(OC)_3MoPtH(PPh_3)]$.[10]

Table 3. Selected ^{1}H n.m.r. data[a]

Complex	
(1)	3.69 [ddd, 2 H, CH_2, $J(P_AH)$ 9, $J(P_BH)$ 9, $J(P_CH)$ 1, J(PtH) 40]
(2)	6.13 [dd, 1 H, CH_2, J(PH) 30 and 13]
	5.99 [dd, 1 H, CH_2, J(PH) 24 and 15]
(3)[b]	3.63 [ddd, 2 H, CH_2, J(PH) 9, 9, and 1, J(PtH) 40]
	2.28 (s, 3 H, CH_3)
(4)	3.50 [dd, 2 H, CH_2, J(PH) 10 and 10, J(PtH) 22]
	−5.53 [ddd, 1 H, PtH, $J(P_AH)$ 11, $J(P_BH)$ 179, $J(P_CH)$ 11, J(PtH) 713]
(5)	8.28 [ddd, 1 H, PtCH, $J(P_BH)$ 7, $J(P_CH)$ 4, J(PtH) 37, J(HH) 7]
	4.70 (br, 1 H, CH_2)
	4.40 (br, 1 H, CH_2)
	3.98 [dddd, 1 H, C(O)CH, $J(P_AH)$ 4, $J(P_BH)$ 8, $J(P_CH)$ 1, J(PtH) 203, J(HH) 7]
(6a)	4.51 (br, 2 H, CH_2)
	3.92 [dd, 1 H, CH, J(PH) 8 and 3, J(PtH) 189]
	2.20 [d, 3 H, CH_3, J(PH) 6, J(PtH) 31]
(6b)	7.95 [dd, 1 H, CH, J(PH) 8 and 4, J(PtH) 35]
	4.65 (br, 1 H, CH_2)
	4.44 (br, 1 H, CH_2)
	1.64 (s, 3 H, CH_3)
(7a)	5.05 [dd, 1 H, CH, $J(P_AH)$ 3, $J(P_BH)$ 8, J(PtH) 201]
	4.85 [AB, 1 H, CH_2, J(HH) 13]
	4.45 [AB, 1 H, CH_2, J(HH) 13]
	2.10 (s, 3 H, CH_3)
(7b)	9.00 [dd, 1 H, CH, $J(P_BH)$ 7, $J(P_CH)$ 4, J(PtH) 27]
	4.76 (br, 1 H, CH_2)
	4.69 (br, 1 H, CH_2)
	2.05 (s, 3 H, CH_3)
(8)	8.57 [dd, 1 H, CH, J(PH) 5 and 7, J(PtH) 28]
	5.38 [dd, 1 H, CH_2, J(PH) 29 and 17]
	5.18 [dd, 1 H, CH_2, J(PH) 28 and 16]
	2.15 (s, 3 H, CH_3)
(9)	8.42 [dd, 1 H, CH, J(PH) 7 and 4, J(PtH) 28]
	4.60 (br, 2 H, CH_2)
(10)	8.04 [dd, 1 H, CH, J(PH) 8 and 4, J(PtH) 32]
	4.50 (br, 2 H, PCH_2P)
	3.05 (br, 3 H, CH_3)
	2.22 (s, 2 H, CH_2N)
(11)[b]	8.13 [dd, 1 H, CH, J(PH) 8 and 4, J(PtH) 34]
	5.30 [dd, 1 H, C=CH_2, J(PH) 23 and 17]
	5.08 [dd, 1 H, C=CH_2, J(PH) 24 and 16]
	2.87 (br, 3 H, CH_3)
	2.30 (s, 2 H, CH_2N)
(12)	8.11 [dd, 1 H, CH, J(PH) 8 and 5, J(PtH) 27]
	4.74 (br, 1 H, CH_2)
	4.49 (br, 1 H, CH_2)
	1.13 (s, 6 H, CH_3)
(13)	8.14 [dd, 1 H, C(O)CH, J(PH) 8 and 4, J(PtH) 32]
	5.33 [dd, 1 H, C=CH_2, J(PH) 30 and 17]
	5.10 [dd, 1 H, C=CH_2, J(PH) 28 and 16]
	3.75 (br, 2 H, CH_2CH)
	3.51 [t, 1 H, CH_2CH, J(HH) 6]
(15)	9.01 [dd, 1 H, CH=CH_2, J(HH) 14 and 9]
	4.65 [AB, 1 H, CH_2, J(HH) 15]
	4.35 [AB, 1 H, CH_2, J(HH) 15]
	4.30 [d, 1 H, CH=CH_2, J(HH) 9]
	4.23 [d, 1 H, CH=CH_2, J(HH) 14]
(16)	4.50 [AB, 1 H, CH_2, J(HH) 15]
	4.43 [AB, 1 H, CH_2, J(HH) 15]
	3.99 (s, 1 H, CMe=CH_2)
	3.90 (s, 1 H, CMe=CH_2)
	2.27 (s, 3 H, CH_3)
(17)	4.51 [AB, 1 H, CH_2, J(HH) 14]
	4.38 [AB, 1 H, CH_2, J(HH) 14]
	4.32 [d, 1 H, CR=CH_2, J(HH) 2]
	3.70 [d, 1 H, CR=CH_2, J(HH) 2]
	2.37 (s, 3 H, CH_3)
(18)	6.21 (s, 1 H, C=CH_2)
	6.19 (s, 1 H, C=CH_2)
	4.42 (s, 1 H, CR=CH_2)
	3.78 (s, 1 H, CR=CH_2)
	2.35 (s, 3 H, CH_3)
(19)	3.83 [dd, 2 H, CH_2, J(PH) 11 and 11, J(PtH) 39]
	3.81 (s, 3 H, CH_3)
	3.69 (s, 3 H, CH_3)
(20)	3.75 [dd, 2 H, CH_2, J(PH) 10 and 10, J(PtH) 48]

[a] Recorded in $CDCl_3$ or CD_2Cl_2 solution at 20 °C and 400 MHz. Chemical shifts (δ) in p.p.m. (±0.01 p.p.m.) relative to $SiMe_4$, coupling constants (J) in Hz (±0.3Hz). ^{31}P-^{1}H Coupling constants are quoted only when resolved and are specifically assigned (*i.e.* to P_A, P_B, or P_C) only when confirmed by double-irradiation experiments; P_A and P_B refer to the dppm or vdpp phosphorus atoms bonded to iron and platinum, respectively, P_C to the triphenylphosphine phosphorus atom. [b] 100-MHz Spectra.

Treatment of a dichloromethane solution of complex (**1**) with ethyne quantitatively yielded a new bimetallic (^{31}P-{^{1}H} n.m.r. evidence) formulated as $[(OC)_2Fe(\mu\text{-dppm})\{\mu\text{-}C(O)C_2H_2\}Pt(PPh_3)]$ (**5**) and characterised by elemental analysis, i.r., ^{31}P-{^{1}H}, and ^{1}H n.m.r. spectroscopy (see Tables for details). In addition, the structure of (**5**) has been determined by *X*-ray crystallography (see below). The ^{31}P-{^{1}H} n.m.r. spectrum was similar to that of complex (**1**) indicating that the phosphine backbone was unchanged (data in Table 2). The ^{1}H n.m.r. spectrum showed two mutually coupled resonances, J(HH) = 7 Hz, assigned to the co-ordinated ethyne protons. The low-field resonance at *ca.* 8 p.p.m. with associated ^{195}Pt satellites, J(PtH) = 37 Hz, was assigned to the ethyne proton R^1, *gem* to platinum, whereas the higher-field resonance at *ca.* 4 p.p.m., also with ^{195}Pt satellites, J(PtH) = 203 Hz, was assigned to the proton R^2, *trans* to platinum. The i.r. spectrum, in the carbonyl region, showed two bands attributable to terminal carbonyl ligands and a third band at very low energy (1 690 cm^{-1}) assigned to a ketonic carbonyl.

Crystal Structure of $[(OC)_2Fe(\mu\text{-dppm})\{\mu\text{-}C(O)C_2H_2\}Pt(PPh_3)]$ (**5**).—Complex (**5**) was crystallised by slow evaporation of a dichloromethane–n-hexane (1:3) solution. The structure is shown in Figure 3 and selected intramolecular

Table 4. Selected distances (pm) and angles (°) between interatomic vectors for $[(OC)_3Fe(\mu\text{-dppm})(\mu\text{-CO})Pt(PPh_3)]$ (**1**)

Fe–Pt	257.9(4)		
P(1)–Fe	225.2(3)	P(2)–Pt	234.7(3)
P(3)–Pt	226.9(3)	C(1)–Fe	176.9(4)
C(2)–Fe	174.1(8)	C(3)–Fe	178.4(8)
C(4)–Fe	201.2(7)	C(4)–Pt	199.2(7)
C(1)–O(1)	114.0(7)	C(2)–O(2)	115.4(8)
C(3)–O(3)	114.7(7)	C(4)–O(4)	116.7(7)
P(1)–C(13)	183.9(7)	P(2)–C(13)	184.6(7)
P(2)–Pt–Fe	94.3	P(3)–Pt–Fe	148.3
P(3)–Pt–P(2)	115.6	C(4)–Pt–Fe	50.3(2)
C(4)–Pt–P(2)	144.2(1)	C(4)–Pt–P(3)	100.2(2)
P(1)–Fe–Pt	97.8	C(1)–Fe–Pt	89.3(3)
C(1)–Fe–P(1)	86.4(3)	C(2)–Fe–Pt	152.7(2)
C(2)–Fe–P(1)	109.2(3)	C(2)–Fe–C(1)	96.2(4)
C(3)–Fe–Pt	77.0(3)	C(3)–Fe–P(1)	94.8(3)
C(3)–Fe–C(1)	166.3(3)	C(3)–Fe–C(2)	96.4(4)
C(4)–Fe–Pt	49.6(1)	C(4)–Fe–P(1)	146.6(1)
C(4)–Fe–C(1)	86.0(3)	C(4)–Fe–C(2)	104.0(4)
C(4)–Fe–C(3)	85.6(3)	C(13)–P(1)–Fe	109.7(3)
C(13)–P(2)–Pt	108.2(3)	O(1)–C(1)–Fe	178.8(6)
O(2)–C(2)–Fe	178.4(6)	O(3)–C(3)–Fe	177.9(5)
Fe–C(4)–Pt	80.2(3)	O(4)–C(4)–Pt	142.6(4)
O(4)–C(4)–Fe	137.1(4)	P(2)–C(13)–P(1)	112.7(3)

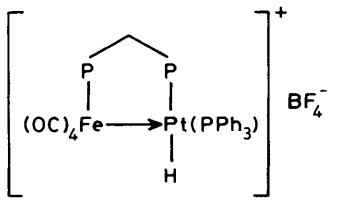

(4) P P = dppm

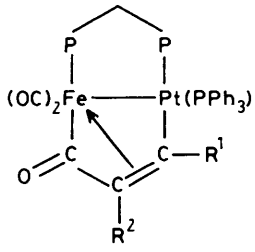

(5)	$R^1 = R^2 = H$	dppm
(6a)	$R^1 = Me$, $R^2 = H$	dppm
(6b)	$R^1 = H$, $R^2 = Me$	dppm
(7a)	$R^1 = C_6H_4Me\text{-}4$, $R^2 = H$	dppm
(7b)	$R^1 = H$, $R^2 = C_6H_4Me\text{-}4$	dppm
(8)	$R^1 = H$, $R^2 = C_6H_4Me\text{-}4$	vdpp
(9)	$R^1 = H$, $R^2 = Ph$	dppm
(10)	$R^1 = H$, $R^2 = CH_2NHMe$	dppm
(11)	$R^1 = H$, $R^2 = CH_2NHMe$	vdpp
(12)	$R^1 = H$, $R^2 = CMe_2OH$	dppm
(13)	$R^1 = H$, $R^2 = CH_2CH_2OH$	vdpp
(14)	$R^1 = H$, $R^2 = CO_2Me$	dppm

distances and angles are in Table 5. The Fe and Pt moieties are linked by a single dppm bridge to give a five-membered FePCPPt ring. The Fe–Pt distance of 259.7(4) pm indicates a metal–metal bond and is close to that found in complex (**1**). Also bridging the metal centres is a species derived from the combination of an ethyne molecule and carbon monoxide generating a dimetallacyclopentenone ring. The $C_2H_2(CO)$ moiety is σ-bonded to platinum and η^3-bonded to iron, similar to that reported for the $C_2Ph_2(CO)$ ligand in the related complex $[Ru_2(CO)(\mu\text{-}CO)\{\mu\text{-}C(O)C_2Ph_2\}(\eta^5\text{-}C_5H_5)_2]$.[11] The relevant bond lengths and angles pertaining to these moieties are very similar and hence a detailed discussion seems inappropriate.

Treatment of complex (**1**) with propyne gave, after several hours, $[(OC)_2Fe(\mu\text{-}dppm)\{\mu\text{-}C(O)CHCMe\}Pt(PPh_3)]$ (**6a**), quantitatively [$^{31}P\text{-}\{^1H\}$ n.m.r. evidence]. The ^1H n.m.r. spectrum showed a resonance at 3.92 p.p.m. with $J(PtH) = 189$ Hz indicating the acetylenic proton to be in position R^2 and *trans* to the platinum. When a benzene solution of (**6a**) was heated for 2 h a quantitative isomerisation [$^{31}P\text{-}\{^1H\}$ n.m.r. evidence] to $[(OC)_2Fe(\mu\text{-}dppm)\{\mu\text{-}C(O)CMeCH\}Pt(PPh_3)]$ (**6b**) resulted. At 20 °C this isomerisation was very slow, *i.e.* after several days less than 10% conversion had occurred. The ^1H n.m.r. spectrum of (**6b**) showed a resonance at 7.95 p.p.m. with $J(PtH) = 35$ Hz indicating that the acetylenic proton was now in position R^1 and geminal to the platinum.

Table 5. Selected distances (pm) and angles (°) between interatomic vectors for $[(OC)_2Fe(\mu\text{-}dppm)\{\mu\text{-}C(O)C_2H_2\}Pt(PPh_3)]$ (**5**)

Fe–Pt	259.7(4)	P(1)–Pt	227.7(4)
P(3)–Pt	226.8(4)	C(3)–Pt	276.0(10)
C(5)–Pt	202.2(9)	P(2)–Fe	220.5(4)
C(1)–Fe	176.3(11)	C(2)–Fe	174.4(10)
C(3)–Fe	191.3(9)	C(4)–Fe	209.5(9)
C(5)–Fe	211.4(9)	C(13)–P(1)	185.2(9)
C(13)–P(2)	183.3(9)	O(1)–C(1)	116.1(13)
O(2)–C(2)	114.7(11)	O(3)–C(3)	121.3(10)
C(4)–C(3)	145.1(12)	C(5)–C(4)	140.8(12)
P(1)–Pt–Fe	101.6(2)	P(3)–Pt–Fe	151.5(1)
P(3)–Pt–P(1)	106.3(2)	C(3)–Pt–Fe	41.7(1)
C(5)–Pt–Fe	52.7(3)	C(5)–Pt–P(1)	152.5(2)
C(5)–Pt–P(3)	98.8(3)	P(2)–Fe–Pt	88.5(2)
C(1)–Fe–Pt	95.7(4)	C(1)–Fe–P(2)	103.0(4)
C(2)–Fe–Pt	165.6(3)	C(2)–Fe–P(2)	97.1(3)
C(2)–Fe–C(1)	96.0(5)	C(3)–Fe–Pt	73.7(3)
C(3)–Fe–P(2)	96.2(3)	C(3)–Fe–C(1)	157.8(4)
C(3)–Fe–C(2)	92.4(4)	C(4)–Fe–Pt	74.1(3)
C(4)–Fe–P(2)	137.6(2)	C(4)–Fe–C(1)	116.7(5)
C(4)–Fe–C(2)	93.0(4)	C(4)–Fe–C(3)	42.1(3)
C(5)–Fe–Pt	49.5(2)	C(5)–Fe–P(2)	137.9(2)
C(5)–Fe–C(1)	87.0(5)	C(5)–Fe–C(2)	122.8(4)
C(5)–Fe–C(3)	71.3(4)	C(5)–Fe–C(4)	39.1(3)
C(13)–P(1)–Pt	104.4(3)	C(13)–P(2)–Fe	114.8(3)
P(2)–C(13)–P(1)	109.4(5)	O(1)–C(1)–Fe	176.1(8)
O(2)–C(2)–Fe	176.0(7)	Fe–C(3)–Pt	64.6(3)
O(3)–C(3)–Fe	148.3(6)	C(4)–C(3)–Fe	75.7(5)
C(4)–C(3)–O(3)	135.3(7)	C(3)–C(4)–Fe	62.2(5)
C(5)–C(4)–Fe	71.2(5)	C(5)–C(4)–C(3)	110.7(7)
Fe–C(5)–Pt	77.8(4)	C(4)–C(5)–Pt	111.5(6)
C(4)–C(5)–Fe	69.7(5)		

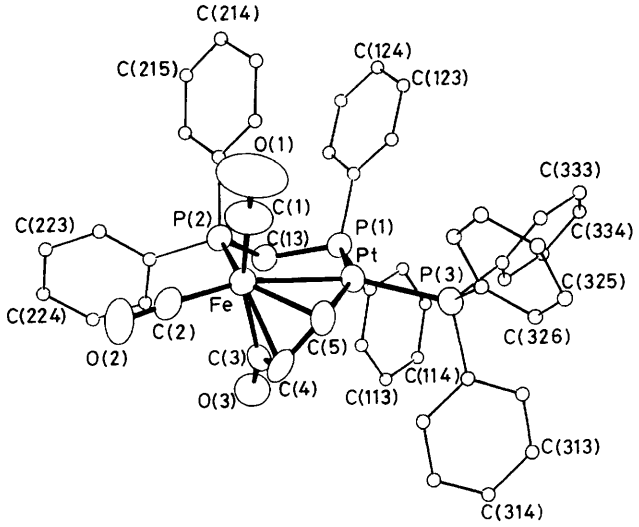

Figure 3. Molecular structure of $[(OC)_2Fe(\mu\text{-}dppm)\{\mu\text{-}C(O)C_2H_2\}Pt(PPh_3)]$ (**5**) showing the principal atomic numbering

Treatment of complex (**1**) with *p*-tolylacetylene gave $[(OC)_2Fe(\mu\text{-}dppm)\{\mu\text{-}C(O)CHC(C_6H_4Me\text{-}4)\}Pt(PPh_3)]$ (**7a**) after 3 h. Characterisation was as for (**5**) and (**6a**). Complex (**7a**) isomerised rapidly in solution (48 h at 20 °C) to give $[(OC)_2Fe(\mu\text{-}dppm)\{\mu\text{-}C(O)C(C_6H_4Me\text{-}4)CH\}Pt(PPh_3)]$ (**7b**), which was also prepared by refluxing (**1**) with *p*-tolylacetylene in benzene for 2 h. Presumably, the isomer which is favoured under given conditions can be explained by kinetic *vs.* thermodynamic

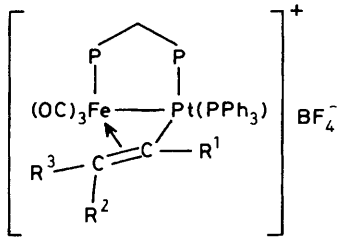

(15) $R^1 = R^2 = R^3 = H$ dppm

(16) $R^1 = Me, R^2 = R^3 = H$ dppm

(17) $R^1 = C_6H_4Me\text{-}4, R^2 = R^3 = H$ dppm

(18) $R^1 = C_6H_4Me\text{-}4, R^2 = R^3 = H$ vdpp

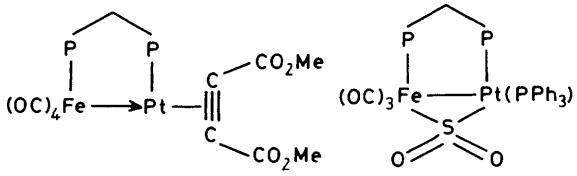

(19) P P = dppm (20) P P = dppm

control and the rate of the isomerisation (**6a**) ⟶ (**6b**) is smaller than for (**7a**) ⟶ (**7b**); possibly steric effects provide the driving force and *p*-tolyl is more bulky than methyl.

These reactions, although giving similar products to those reported by Knox and co-workers [12] with Fe_2, Ru_2, and FeRu bimetallics, differ in that the FePt system does not require photolytic activation. It was demonstrated that the heteronuclear FeRu system was more reactive than either of the homonuclear analogues and our results show that the FePt centre appears to possess an even higher reactivity. Many of the reactions reported by Knox and co-workers of Fe_2, Ru_2, and FeRu complexes with alkynes gave products containing mixtures of isomers that appeared not to interconvert. The favoured isomers of the Knox compounds contained $\overline{M_2C(H)C(R)CO}$ rings, *i.e.* with the substituent in the R^2 position because of greater steric hindrance in the R^1 position. Presumably the mild conditions required in our FePt system make possible the isolation of the more sterically crowded isomer, *i.e.* with the substituent in the R^1 position.

Several analogues of complex (**7b**) with various R groups were also prepared directly from (**1**), *i.e.* (**9**), (**10**), (**12**), and (**14**), and analogues with vdpp from (**2**), *i.e.* (**8**), (**11**), and (**13**). Characterising data for these complexes are collected in Tables 1—3. All the alkyne complexes were stable in air, both in solution and in the solid state.

$^{31}P\text{-}\{^1H\}$ N.m.r. and i.r. studies of the reaction between complex (**1**) and *p*-tolylacetylene (1 mol equivalent or an excess) indicated that $[Fe(CO)_4(dppm\text{-}P)]$ was produced as an intermediate, *viz.* the $^{31}P\text{-}\{^1H\}$ n.m.r. spectrum showed two doublets at 66.7 and −25.2 p.p.m., $J(PP) = 78$ Hz, and on addition of more $[Fe(CO)_4(dppm\text{-}P)]$ these two doublets increased in intensity. The i.r. spectrum of the reaction solution showed a high-energy band at 2 054 cm^{-1}. This band disappeared on completion of the reaction. In the $^{31}P\text{-}\{^1H\}$ n.m.r. spectrum the resonance due to PPh_3 was only about half the intensity one would expect, even at −80 °C. No satisfactory explanation is offered for this observation but we tentatively suggest that reaction proceeds by attack of $[Fe(CO)_4(dppm\text{-}P)]$ on $[Pt(alkyne)_2(PPh_3)]$ or some related platinum species. All the alkynes used underwent analogous reactions involving similar intermediates.

Table 6. Selected distances (pm) and angles (°) between interatomic vectors for $[(OC)_3Fe(\mu\text{-dppm})(\mu\text{-CMe=CH}_2)Pt(PPh_3)][BF_4]$ (**16**)

Fe–Pt	263.0(5)	P(2)–Pt	240.7(5)
P(3)–Pt	225.0(6)	C(2)–Pt	233.8(16)
C(5)–Pt	202.5(14)	P(1)–Fe	231.0(6)
C(1)–Fe	176.3(17)	C(2)–Fe	181.3(16)
C(3)–Fe	175.5(17)	C(4)–Fe	223.5(16)
C(5)–Fe	220.1(15)	C(13)–P(1)	180.4(15)
C(13)–P(2)	190.7(16)	O(1)–C(1)	116.2(19)
O(2)–C(2)	117.4(20)	O(3)–C(3)	114.3(19)
C(5)–C(4)	139.6(18)	C(6)–C(5)	148.1(19)
P(2)–Pt–Fe	94.0(2)	P(3)–Pt–Fe	158.3(1)
P(3)–Pt–P(2)	107.0(2)	C(2)–Pt–Fe	42.3(3)
C(2)–Pt–P(2)	85.4(5)	C(2)–Pt–P(3)	132.5(4)
C(5)–Pt–Fe	54.6(5)	C(5)–Pt–P(2)	146.5(4)
C(5)–Pt–P(3)	105.6(5)	C(5)–Pt–C(2)	78.2(6)
P(1)–Fe–Pt	96.6(2)	C(1)–Fe–Pt	108.9(6)
C(1)–Fe–P(1)	88.3(6)	C(2)–Fe–Pt	60.2(6)
C(2)–Fe–P(1)	92.6(6)	C(2)–Fe–C(1)	169.1(7)
C(3)–Fe–Pt	155.9(5)	C(3)–Fe–P(1)	95.8(6)
C(3)–Fe–C(1)	92.0(8)	C(3)–Fe–C(2)	98.7(8)
C(4)–Fe–Pt	76.3(5)	C(4)–Fe–P(1)	171.8(4)
C(4)–Fe–C(1)	98.0(7)	C(4)–Fe–C(2)	80.2(7)
C(4)–Fe–C(3)	89.3(7)	C(5)–Fe–Pt	48.6(3)
C(5)–Fe–P(1)	139.5(3)	C(5)–Fe–C(1)	85.9(7)
C(5)–Fe–C(2)	86.4(7)	C(5)–Fe–C(3)	124.4(7)
C(5)–Fe–C(4)	36.7(4)	C(13)–P(1)–Fe	112.9(6)
C(13)–P(2)–Pt	106.9(5)	P(2)–C(13)–P(1)	113.1(8)
O(1)–C(1)–Fe	175.4(14)	Fe–C(2)–Pt	77.5(6)
O(2)–C(2)–Pt	112.5(11)	O(2)–C(2)–Fe	169.7(13)
O(3)–C(3)–Fe	178.0(15)	C(5)–C(4)–Fe	70.3(9)
Fe–C(5)–Pt	76.8(5)	C(4)–C(5)–Pt	123.1(10)
C(4)–C(5)–Fe	73.0(9)	C(6)–C(5)–Pt	119.3(10)
C(6)–C(5)–Fe	121.7(10)	C(6)–C(5)–C(4)	117.6(13)

Addition of $HBF_4{\cdot}OEt_2$ to a dichloromethane solution of complex (**5**) gave the μ-vinyl cation $[(OC)_3Fe(\mu\text{-dppm})(\mu\text{-CH=CH}_2)Pt(PPh_3)][BF_4]$ (**15**) in a carbon-carbon bond-cleavage reaction similar to those reported by Knox and co-workers [12,13] in Fe_2, Ru_2, and FeRu systems. The μ-vinyl ^1H resonances (Table 3) are of the usual form with coupling constants 14 and 9 Hz which are expected for *J*(*trans*) and *J*(*cis*), respectively; *J*(*geminal*) was not resolved. The signal at 9.01 p.p.m. is assigned to the vinylic CH proton on the basis of the couplings, and the signals at 4.30 and 4.23 p.p.m. to the methylenic protons *cis* and *trans* to it. The low-field signal is characteristic of a proton attached to a μ-carbene carbon atom.[14] Protonation of (**6a**) or (**6b**) led to the formation of the monosubstituted vinyl complex $[(OC)_3Fe(\mu\text{-dppm})(CMe=CH_2)Pt(PPh_3)][BF_4]$ (**16**) and, similarly, protonation of (**7b**) or (**8**) gave the structurally analogous complexes (**17**) and (**18**) respectively. Complexes (**16**)—(**18**) were readily identified as of the $\mu\text{-CR=CH}_2$ type by the absence of a low-field ^1H n.m.r. signal due to μ-CH. The exclusive formation of the $\mu\text{-CR=CH}_2$ type cations is worth comparing with previous studies on Fe_2, Ru_2, and FeRu systems.[12,13] With Fe_2 and FeRu, protonation of the dimetallacyclopentenone complexes derived from propyne gave the μ-CH=C(Me)H cation as the favoured species. However, with Ru_2 the $\mu\text{-CMe=CH}_2$ cation was favoured and further the $\mu\text{-CPh=CH}_2$ cation was formed exclusively on protonation of the dimetallacyclopentenone derived from phenylacetylene. Therefore, the results for the FePt system appear to resemble most closely those previously reported for Ru_2 complexes. Clearly, vinyl isomerisation must be important in providing a route to thermodynamically stable species.

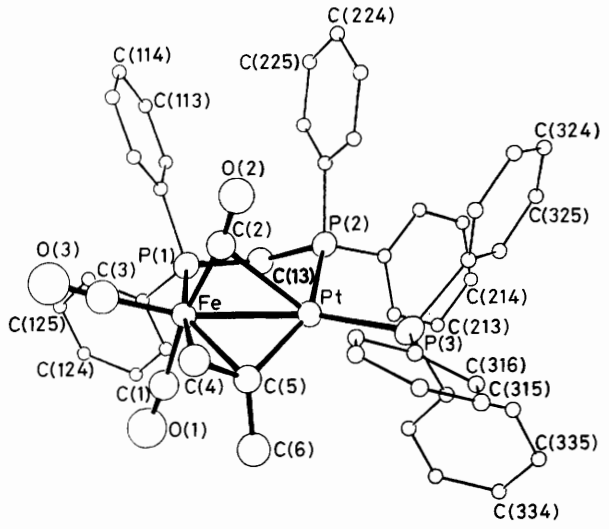

Figure 4. Molecular structure of $[(OC)_3Fe(\mu\text{-dppm})(\mu\text{-CMe=CH}_2)\text{-}Pt(PPh_3)][BF_4]$ (**16**) showing the principal atomic numbering

The i.r. spectra of the μ-vinyl cations (**15**)—(**18**) were similar in the carbonyl region and each showed three bands assigned to metal carbonyl ligands.

An *X*-ray diffraction study was undertaken on the $\mu\text{-CMe=CH}_2$ complex and is described in detail below.

Crystal Structure of $[(OC)_3Fe(\mu\text{-dppm})(\mu\text{-CMe=CH}_2)Pt(PPh_3)][BF_4]$ (**16**).—The complex (**16**) was crystallised from acetone–diethyl ether (1:3) solution. The structure is shown in Figure 4 and selected intramolecular distances and angles are in Table 6. In the cation the Fe and Pt moieties are linked by a single dppm bridge, to give a FePCPPt ring. The Fe–Pt distance of 263.0(5) pm indicates a metal–metal bond and is close to those found in complexes (**1**) and (**5**). Also bridging the metal centres is the μ-vinyl moiety $CMe\text{=}CH_2$. The Fe–C(4) distance, 223.5(16) pm, and the Fe–C(5) distance, 220.1(15) pm, indicate an almost symmetric disposition for the co-ordinated 'ethylenic fragment'. The μ-carbene type carbon atom C(5) is, however, asymmetrically bridging the metal centres, *viz.* C(5)–Pt 202.5(14) and C(5)–Fe 220.1(15) pm. The Pt–C(2) distance of 233.8(16) pm and the angles Fe–C(2)–O(2) 169.7(13) and Pt–C(2)–O(2) 112.5(11)° suggest the presence of a very weakly semi-bridging carbonyl ligand. The structure of the cation can be compared with that of the related complex $[Fe_2(CO)_2(\mu\text{-CO})(\mu\text{-CHCH}_2)(\eta^5\text{-}C_5H_5)_2][BF_4]$.[15]

In contrast to the reaction between complex (**1**) and alkynes discussed above, treatment of (**1**) with dimethyl acetylenedicarboxylate gave the complex $[(OC)_4Fe(\mu\text{-dppm})Pt(MeO_2CC\equiv CCO_2Me)]$ (**19**) resulting from displacement of the PPh_3 ligand by the activated alkyne. It was characterised by elemental analysis and i.r., $^{31}P\text{-}\{^1H\}$, and ^1H n.m.r. spectroscopy. The i.r. spectrum showed no bands which could be assigned to bridging metal carbonyl ligands but showed a strong band at 1 695 cm^{-1} assigned to the carbonyl ligands of the co-ordinated alkyne. The $^{31}P\text{-}\{^1H\}$ n.m.r. spectrum showed an AX pattern with the low-field resonance showing weak coupling to ^{195}Pt [*J*(PtP) 126 Hz] and the high-field resonance showing strong coupling [*J*(PtP) 1 990 Hz]. These data confirmed the absence of PPh_3 and the presence of a single bridging dppm ligand. Complex (**19**) showed no reactivity towards other alkynes, *i.e.* no dimetallacyclopentenone type complexes were formed.

The bridging sulphur dioxide complex $[(OC)_3Fe(\mu\text{-dppm})(\mu\text{-}SO_2)Pt(PPh_3)]$ (**20**) was instantly formed in high yield when SO_2 was bubbled through a dichloromethane solution of (**1**). This SO_2 adduct has i.r., ^1H n.m.r., and $^{31}P\text{-}\{^1H\}$ n.m.r. spectra in accord with a bridging SO_2 ligand having replaced the bridging CO in (**1**). A related diruthenium complex $[Ru_2(CO)_2(\mu\text{-CO})(\mu\text{-}SO_2)(\eta^5\text{-}C_5H_5)_2]$ has been reported.[16]

Experimental

General methods were as previously described in recent papers from this laboratory.[17] The complexes $[Fe(CO)_4(dppm\text{-}P)]$, $[Fe(CO)_4(vdpp\text{-}P)]$,[1] and $[(OC)_3Fe(\mu\text{-dppm})(\mu\text{-CO})PtCl_2]$[4] were prepared by previously described methods.

Preparations.—$[(OC)_3Fe(\mu\text{-dppm})(\mu\text{-CO})Pt(PPh_3)]$ (**1**) *from* $[Fe(CO)_4(dppm\text{-}P)]$ *and* $[Pt(trans\text{-PhCH=CHPh})(PPh_3)_2]$. A mixture of $[Fe(CO)_4(dppm\text{-}P)]$ (1.1 g, 2 mmol) and $[Pt(trans\text{-PhCH=CHPh})(PPh_3)_2]$ (1.8 g, 2 mmol) was stirred in benzene (40 cm^3) for 1 h after which an orange solid had precipitated. The volume of the solution was reduced to *ca.* 10 cm^3 and an excess of light petroleum (b.p. 40—60 °C) was then added. The solid product was isolated by filtration and recrystallised from dichloromethane–light petroleum (b.p. 40—60 °C) to give the desired product as orange prisms. Yield 1.51 g, 75%.

The vdpp analogue (**2**) was similarly prepared as red microcrystals in 79% yield using $[Fe(CO)_4(vdpp\text{-}P)]$.

Complex (**1**) *from* $[(OC)_3Fe(\mu\text{-dppm})(\mu\text{-CO})PtCl_2]$ *and* $NaBH_4$–PPh_3. A solution of $NaBH_4$ (0.038 g, 1 mmol) in ethanol (5 cm^3) was added dropwise to a stirred solution of $[(OC)_3Fe(\mu\text{-dppm})(\mu\text{-CO})PtCl_2]$ (0.15 g, 0.18 mmol) and PPh_3 (0.048 g, 0.18 mmol) in dichloromethane (20 cm^3). The dark red solution was stirred for 0.5 h then the solvents were removed under reduced pressure. Recrystallisation of the residue from dichloromethane–light petroleum (b.p. 40—60 °C) gave the desired product as orange prisms. Yield 0.14 g, 77%.

The tri-*p*-tolylphosphine analogue (**3**) was prepared similarly as red-brown microcrystals, in 36% yield.

$[(OC)_4Fe(\mu\text{-dppm})PtH(PPh_3)][BF_4]$ (**4**). An excess of $HBF_4\cdot OEt_2$ (0.25 cm^3) was added to a solution of $[(OC)_3Fe(\mu\text{-dppm})(\mu\text{-CO})Pt(PPh_3)]$ (**1**) (0.30 g, 0.30 mmol) in dichloromethane (10 cm^3). After 5 min the solvent was removed under reduced pressure and the residue triturated with diethyl ether to give the desired product as yellow-brown microcrystals. Yield 0.29 g, 90%.

$[(OC)_2Fe(\mu\text{-dppm})\{\mu\text{-}C(O)C_2H_2\}Pt(PPh_3)]$ (**5**). Acetylene was bubbled through a solution of complex (**1**) (0.30 g, 0.30 mmol) in dichloromethane (4 cm^3) for 20 min. The flask was stoppered and the mixture set aside for 18 h. The solvent was removed under reduced pressure and the residue recrystallised from dichloromethane–n-hexane to give the desired product as orange microcrystals. Yield 0.24 g, 80%.

$[(OC)_2Fe(\mu\text{-dppm})\{\mu\text{-}C(O)CHCMe\}Pt(PPh_3)]$(**6a**).Methylacetylene was bubbled through a solution of complex (**1**) (0.18 g, 0.18 mmol) in dichloromethane (3 cm^3) for 1 min. The flask was stoppered and the mixture set aside for 24 h. The solvent was removed under reduced pressure and the residue recrystallised from dichloromethane–n-hexane to give the desired product as orange microcrystals. Yield 0.13 g, 71%.

$[(OC)_2Fe(\mu\text{-dppm})\{\mu\text{-}C(O)CMeCH\}Pt(PPh_3)]$ (**6b**). The complex (**6a**) (0.10 g, 0.098 mmol) was refluxed in benzene (20 cm^3) for 2 h. The solvent was removed under reduced pressure and the residue recrystallised from dichloromethane–n-hexane to give the desired product as orange microcrystals. Yield 0.07 g, 70%.

$[(OC)_2Fe(\mu\text{-dppm})\{\mu\text{-}C(O)CHC(C_6H_4Me\text{-}4)\}Pt(PPh_3)]$ (**7a**). *p*-Tolylacetylene (0.058 g, 0.5 mmol) was added to a

Table 7. Crystallographic data for complexes (**1**), (**5**), and (**16**)

Crystal data	(1)	(5)	(16)
Formula	$C_{53}H_{43}FeO_4P_3Pt$	$C_{48}H_{39}FeO_3P_3Pt$	$C_{52}H_{48}BF_4FeO_4P_3Pt$
M	1 087.77	1 007.69	1 167.60
System	Triclinic	Orthorhombic	Monoclinic
a/pm	1 177.3(2)	1 898.9(4)	2 321.3(3)
b/pm	1 198.4(1)	1 828.3(3)	1 091.2(2)
c/pm	1 776.5(1)	2 414.4(5)	1 962.6(2)
α/°	103.34(1)	—	—
β/°	107.81(1)	—	98.48(1)
γ/°	91.76(1)	—	—
U/nm^3	2.305	8.384	4.917
Z	2	8	4
Space group	$P\bar{1}$	$Pbca$	Cc
D_c/g cm^{-3}	1.57	1.60	1.58
μ/cm^{-1}	33.36	36.64	31.16
$F(000)$	1 092	4 000	2 292
Data collection			
Scan type	ω—2θ	ω—2θ	ω
Scan width (° + α-doublet splitting)	2.0	2.0	1.0
Scan speeds/° min^{-1}	2.0—29.3	2.0—29.3	2.0—29.3
$2\theta_{min.}$, $2\theta_{max.}$/°	4.0, 45.0	4.0, 45.0	4.0, 47.5
Total data	6 210	6 239	4 074
Unique data	5 904	5 007	3 988
No. observed	5 422	4 163	3 615
Sigma threshold	2.0	1.5	2.0
Refinement			
g	0.0004	0.0002	0.0003
R	0.0257	0.0381	0.0460
R'	0.0264	0.0327	0.0506
No. of parameters	443	426	204

Table 8. Non-hydrogen atom co-ordinates ($\times 10^4$) for compound (**1**)

Atom	x	y	z	Atom	x	y	z
Pt	3 265.1(2)	−1 131.0(2)	2 238.3(1)	C(216)	5 937(3)	−2 680(3)	3 762(2)
Fe	3 593(1)	1 070(1)	2 854.9(4)	C(221)	6 034(2)	−1 233(3)	1 870(2)
P(1)	5 607(1)	1 249(1)	3 398(1)	C(222)	5 304(2)	−1 284(3)	1 075(2)
P(2)	5 321(1)	−1 355(1)	2 629(1)	C(223)	5 819(2)	1 162(3)	484(2)
P(3)	2 031(1)	−2 697(1)	1 365(1)	C(224)	7 064(2)	−990(3)	687(2)
C(1)	3 558(5)	835(5)	3 796(4)	C(225)	7 794(2)	−940(3)	1 481(2)
O(1)	3 519(5)	696(5)	4 403(3)	C(226)	7 279(2)	−1 061(3)	2 073(2)
C(2)	3 099(6)	2 434(5)	2 997(4)	C(311)	1 119(3)	−3 472(3)	1 792(2)
O(2)	2 745(6)	3 327(5)	3 081(4)	C(312)	1 120(3)	−4 655(3)	1 724(2)
C(3)	3 591(5)	939(5)	1 833(4)	C(313)	441(3)	−5 199(3)	2 085(2)
O(3)	3 556(4)	864(4)	1 169(2)	C(314)	−238(3)	−4 560(3)	2 514(2)
C(4)	2 068(5)	−15(4)	2 342(3)	C(315)	−239(3)	−3 377(3)	2 582(2)
O(4)	1 044(3)	44(3)	2 228(3)	C(316)	440(3)	−2 833(3)	2 221(2)
C(111)	6 176(3)	2 177(3)	4 443(2)	C(321)	912(2)	−2 302(3)	524(2)
C(112)	5 941(3)	3 327(3)	4 550(2)	C(322)	−275(2)	−2 807(3)	208(2)
C(113)	6 280(3)	4 062(3)	5 335(2)	C(323)	−1 068(2)	−2 528(3)	−469(2)
C(114)	6 854(3)	3 648(3)	6 012(2)	C(324)	−673(2)	−1 745(3)	−831(2)
C(115)	7 089(3)	2 498(3)	5 904(2)	C(325)	514(2)	−1 240(3)	−516(2)
C(116)	6 750(3)	1 763(3)	5 120(2)	C(326)	1 306(2)	−1 519(3)	161(2)
C(121)	6 616(3)	1 785(3)	2 919(2)	C(331)	2 680(3)	−3 866(3)	823(2)
C(122)	6 152(3)	2 228(3)	2 239(2)	C(332)	2 235(3)	−4 302(3)	−24(2)
C(123)	6 914(3)	2 572(3)	1 848(2)	C(333)	2 734(3)	−5 218(3)	−405(2)
C(124)	8 140(3)	2 474(3)	2 137(2)	C(334)	3 678(3)	−5 697(3)	62(2)
C(125)	8 604(3)	2 031(3)	2 817(2)	C(335)	4 123(3)	−5 261(3)	909(2)
C(126)	7 843(3)	1 687(3)	3 208(2)	C(336)	3 624(3)	−4 345(3)	1 289(2)
C(13)	6 106(4)	−156(4)	3 523(3)	C(1S)	578(10)	1 054(9)	5 519(7)
C(211)	5 968(3)	−2 567(3)	3 004(2)	C(2S)	775(9)	643(9)	4 744(7)
C(212)	6 444(3)	−3 397(3)	2 530(2)	C(3S)	−169(10)	428(10)	5 741(6)
C(213)	6 890(3)	−4 340(3)	2 816(2)	C(4S)	539(13)	5 726(13)	4 764(9)
C(214)	6 859(3)	−4 453(3)	3 575(2)	C(5S)	727(13)	4 740(13)	4 519(9)
C(215)	6 382(3)	−3 623(3)	4 048(2)	C(6S)	−101(13)	6 131(13)	5 234(9)

Table 9. Non-hydrogen atom co-ordinates ($\times 10^4$) for compound (**5**)

Atom	*x*	*y*	*z*	Atom	*x*	*y*	*z*
Pt	1 943.8(1)	3 566.7(1)	3 785.5(1)	C(225)	4 391(2)	1 479(3)	5 196(2)
Fe	2 497.3(5)	3 579.1(6)	4 768.9(4)	C(226)	3 830(2)	1 747(3)	4 882(2)
P(1)	1 968(1)	2 352(1)	3 579(1)	C(311)	2 264(2)	4 484(2)	2 554(2)
P(2)	2 482(1)	2 373(1)	4 757(1)	C(312)	2 146(2)	4 609(2)	1 991(2)
P(3)	1 564(1)	4 146(1)	3 010(1)	C(313)	2 699(2)	4 829(2)	1 650(2)
C(111)	2 393(3)	2 142(3)	2 924(2)	C(314)	3 372(2)	4 924(2)	1 872(2)
C(112)	3 030(3)	2 497(3)	2 822(2)	C(315)	3 490(2)	4 799(2)	2 434(2)
C(113)	3 367(3)	2 412(3)	2 313(2)	C(316)	2 937(2)	4 579(2)	2 775(2)
C(114)	3 066(3)	1 971(3)	1 905(2)	C(321)	1 048(2)	4 941(2)	3 211(2)
C(115)	2 429(3)	1 616(3)	2 006(2)	C(322)	672(2)	4 890(2)	3 706(2)
C(116)	2 092(3)	1 701(3)	2 515(2)	C(323)	207(2)	5 446(2)	3 858(2)
C(121)	1 202(2)	1 763(3)	3 609(2)	C(324)	118(2)	6 052(2)	3 515(2)
C(122)	539(2)	2 089(3)	3 569(2)	C(325)	493(2)	6 103(2)	3 020(2)
C(123)	−66(2)	1 658(3)	3 591(2)	C(326)	958(2)	5 548(2)	2 868(2)
C(124)	−9(2)	902(3)	3 651(2)	C(331)	989(2)	3 684(2)	2 513(2)
C(125)	653(2)	576(3)	3 690(2)	C(332)	271(2)	3 841(2)	2 492(2)
C(126)	1 259(2)	1 007(3)	3 669(2)	C(333)	−153(2)	3 511(2)	2 092(2)
C(13)	2 614(4)	1 962(4)	4 072(3)	C(334)	142(2)	3 023(2)	1 713(2)
C(211)	1 705(2)	1 864(3)	5 006(2)	C(335)	860(2)	2 866(2)	1 734(2)
C(212)	1 038(2)	2 182(3)	4 973(2)	C(336)	1 284(2)	3 196(2)	2 134(2)
C(213)	446(2)	1 789(3)	5 142(2)	C(1)	1 712(5)	3 801(5)	5 120(4)
C(214)	521(2)	1 078(3)	5 343(2)	O(1)	1 213(4)	3 984(4)	5 361(4)
C(215)	1 187(2)	760(3)	5 376(2)	C(2)	3 050(4)	3 679(4)	5 341(3)
C(216)	1 779(2)	1 153(3)	5 208(2)	O(2)	3 429(4)	3 781(4)	5 703(3)
C(221)	3 206(2)	1 956(3)	5 143(2)	C(3)	3 261(4)	3 691(4)	4 259(3)
C(222)	3 143(2)	1 899(3)	5 717(2)	O(3)	3 771(3)	3 424(3)	4 034(2)
C(223)	3 704(2)	1 632(3)	6 030(2)	C(4)	2 990(4)	4 426(4)	4 332(3)
C(224)	4 328(2)	1 422(3)	5 770(2)	C(5)	2 261(4)	4 450(4)	4 223(3)

Table 10. Non-hydrogen atom co-ordinates ($\times 10^4$) for compound (**16**)

Atom	*x*	*y*	*z*	Atom	*x*	*y*	*z*
Pt	5 000*	2 432.1(3)	0*	C(314)	3 115(4)	1 044(9)	−2 120(5)
Fe	5 930(1)	1 060(3)	−20(1)	C(315)	2 794(4)	1 670(9)	−1 659(5)
P(1)	6 535(2)	2 319(3)	658(2)	C(316)	3 074(4)	2 266(9)	−1 098(5)
P(2)	5 514(2)	4 152(3)	518(2)	C(321)	3 962(4)	4 653(7)	−494(5)
P(3)	4 082(2)	3 039(3)	−250(2)	C(322)	3 956(4)	5 016(7)	−1 176(5)
C(111)	7 081(4)	3 181(9)	275(5)	C(323)	3 939(4)	6 258(7)	−1 344(5)
C(112)	7 429(4)	4 006(9)	662(5)	C(324)	3 927(4)	7 138(7)	−830(5)
C(113)	7 858(4)	4 658(9)	359(5)	C(325)	3 932(4)	6 776(7)	−148(5)
C(114)	7 939(4)	4 485(9)	−331(5)	C(326)	3 950(4)	5 533(7)	20(5)
C(115)	7 591(4)	3 659(9)	−718(5)	C(331)	3 689(4)	2 823(10)	475(4)
C(116)	7 162(4)	3 007(9)	−415(5)	C(332)	3 945(4)	2 172(10)	1 031(4)
C(121)	7 001(5)	1 594(10)	1 402(5)	C(333)	3 640(4)	1 969(10)	1 605(4)
C(122)	6 737(5)	1 300(10)	1 995(5)	C(334)	3 078(4)	2 416(10)	1 623(4)
C(123)	7 054(5)	716(10)	2 535(5)	C(335)	2 822(4)	3 067(10)	1 067(4)
C(124)	7 634(5)	425(10)	2 481(5)	C(336)	3 128(4)	3 271(10)	494(4)
C(125)	7 897(5)	719(10)	1 887(5)	C(1)	5 945(6)	15(13)	666(8)
C(126)	7 580(5)	1 303(10)	1 347(5)	O(1)	5 990(6)	−701(12)	1 106(7)
C(13)	6 152(6)	3 505(12)	1 076(7)	C(2)	5 790(6)	2 239(13)	−662(8)
C(211)	5 200(4)	5 058(8)	1 139(5)	O(2)	5 764(5)	2 915(11)	−1 129(6)
C(212)	4 940(4)	4 434(8)	1 654(5)	C(3)	6 483(7)	274(14)	−397(8)
C(213)	4 686(4)	5 088(8)	2 163(5)	O(3)	6 845(6)	−207(13)	−655(7)
C(214)	4 692(4)	6 366(8)	2 156(5)	C(4)	5 279(6)	88(13)	−726(7)
C(215)	4 951(4)	6 991(8)	1 641(5)	C(5)	5 005(6)	607(11)	−187(6)
C(216)	5 205(4)	6 336(8)	1 132(5)	C(6)	4 720(7)	−235(14)	274(8)
C(221)	5 798(4)	5 257(8)	−31(4)	O(1S)	1 944(6)	787(13)	1 957(8)
C(222)	5 471(4)	5 526(8)	−639(4)	C(1S)	1 633(7)	1 179(15)	2 386(9)
C(223)	5 650(4)	6 448(8)	−1 067(4)	C(2S)	1 349(8)	289(17)	2 785(9)
C(224)	6 156(4)	7 102(8)	−887(4)	C(3S)	1 579(13)	2 498(17)	2 495(16)
C(225)	6 483(4)	6 833(8)	−279(4)	B(1)	5 189(10)	926(22)	2 432(13)
C(226)	6 304(4)	5 911(8)	149(4)	F(1)	5 290(6)	1 454(13)	1 839(7)
C(311)	3 676(4)	2 235(9)	−998(5)	F(2)	4 819(7)	1 569(14)	2 775(8)
C(312)	3 997(4)	1 609(9)	−1 459(5)	F(3)	5 686(8)	664(17)	2 893(10)
C(313)	3 716(4)	1 014(9)	−2 020(5)	F(4)	4 903(9)	−90(21)	2 259(10)

* Co-ordinate fixed.

solution of complex (**1**) (0.20 g, 0.20 mmol) in dichloromethane (3 cm^3). After 3 h the solvent was removed under reduced pressure and the residue recrystallised from dichloromethane–n-hexane to give the desired product as orange microcrystals. Yield 0.15 g, 68%.

$[(OC)_2Fe(\mu\text{-dppm})\{\mu\text{-}C(O)C(C_6H_4Me\text{-}4)CH\}Pt(PPh_3)]$ (**7b**). A mixture of complex (**1**) (0.30 g, 0.30 mmol) and *p*-tolylacetylene (0.087 g, 0.75 mmol) in benzene (20 cm^3) was refluxed for 2 h. The solution was cooled to *ca.* 20 °C and the solvent removed under reduced pressure. The residue was recrystallised from dichloromethane–n-hexane to give the desired product as orange microcrystals. Yield 0.265 g, 80%.

The following complexes were similarly prepared from (**1**) or (**2**) as appropriate (yields in parentheses): (**8**) (65), (**9**) (63), (**10**) (85), (**11**) (76), (**12**) (85), (**13**) (79), and (**14**) (75%).

$[(OC)_3Fe(\mu\text{-dppm})(\mu\text{-}CH{=}CH_2)Pt(PPh_3)][BF_4]$ (**15**). An excess of $HBF_4{\cdot}OEt_2$ (0.25 cm^3) was added to a solution of complex (**5**) (0.10 g, 0.1 mmol) in dichloromethane (3 cm^3). After 2 h the solvent was removed under reduced pressure and the residue triturated with diethyl ether to give the desired product as pale yellow microcrystals. Yield 0.08 g, 73%.

The following complexes were similarly prepared (yields in parentheses): (**16**) from (**6b**) (72), (**17**) from (**7b**) (78), and (**18**) from (**8**) (82%).

$[(OC)_4Fe(\mu\text{-dppm})Pt(MeO_2CC{\equiv}CCO_2Me)]$ (**19**). An excess of $MeO_2CC{\equiv}CCO_2Me$ (0.5 cm^3) was added to a solution of complex (**1**) (0.30 g, 0.30 mmol) in dichloromethane (20 cm^3). After 4 h the solvent was removed under reduced pressure and the residue triturated with diethyl ether to give the desired product as green-brown microcrystals. Yield 0.245 g, 91%.

$[(OC)_3Fe(\mu\text{-dppm})(\mu\text{-}SO_2)Pt(PPh_3)]$ (**20**). Sulphur dioxide was bubbled through a solution of complex (**1**) (0.20 g, 0.20 mmol) in dichloromethane (3 cm^3) for 2 min. Addition of light petroleum (b.p. 60—80 °C) gave the desired product as yellow microcrystals. Yield 0.17 g, 80%.

X-*Ray Crystallography*.—All crystallographic measurements were made on a Nicolet P3/F diffractometer operating in either the ω—2θ scan mode for complexes (**1**) and (**5**) or the ω scan mode for (**16**) using graphite-monochromatised Mo-K_α radiation (λ = 71.069 pm) following a standard procedure described in detail elsewhere.[18] All three data sets were corrected for absorption empirically once their structures had been determined.[19] All three compounds were solved *via* standard heavy-atom methods and refined by full-matrix least squares using the SHELX program system.[20] In all three cases phenyl groups were treated as rigid bodies with idealised hexagonal symmetry (C–C 139.5 pm). For compounds (**1**) and (**5**) all non-hydrogen atoms were assigned anisotropic thermal parameters apart from two 'half' benzene molecules in compound (**1**) (both situated by symmetry centres) which were each refined with an overall isotropic thermal parameter. For both of these complexes the methylene and phenyl hydrogen atoms were included in calculated positions (C–H 108 pm) and an overall isotropic thermal parameter was assigned for each group. For compound (**16**) only the Pt, Fe, and P atoms were assigned anisotropic thermal parameters while all other atoms (including the acetone solvent molecule) were assigned isotropic thermal parameters. No hydrogen atoms were located for this complex. The weighting scheme $w = [\sigma^2(F_o) + g(F_o)^2]^{-1}$ was used for all three compounds in which the parameter g was included in the refinement in order to obtain satisfactory agreement analyses. All relevant crystal data, data-collection, and structure-refinement parameters are listed in Table 7 whilst non-hydrogen atomic co-ordinates for compounds (**1**), (**5**), and (**16**) are given in Tables 8, 9, and 10 respectively.

Additional material available from the Cambridge Crystallographic Data Centre comprises H-atom co-ordinates, thermal parameters, and remaining bond lengths and angles.

Acknowledgements

We thank the S.E.R.C. for support and Johnson Matthey Ltd. for the generous loan of platinum metal salts.

References

1 G. B. Jacobsen, B. L. Shaw, and M. Thornton-Pett, *J. Chem. Soc., Dalton Trans.*, 1987, 1509.
2 G. B. Jacobsen, B. L. Shaw, and M. Thornton-Pett, *J. Chem. Soc., Dalton Trans.*, 1987, 2751.
3 G. B. Jacobsen, B. L. Shaw, and M. Thornton-Pett, *J. Chem. Soc., Chem. Commun.*, 1986, 13.
4 G. B. Jacobsen, B. L. Shaw, and M. Thornton-Pett, *J.Chem. Soc., Dalton Trans.*, 1987, 662.
5 X. L. R. Fontaine, G. B. Jacobsen, B. L. Shaw, and M. Thornton-Pett, *J. Chem. Soc., Chem. Commun.*, in the press.
6 P. A. Wegner, L. F. Evans, and J. Haddock, *Inorg. Chem.*, 1975, **14**, 192.
7 L. J. Farrugia, J. A. K. Howard, P. Mitrprachachon, F. G. A. Stone, and P. Woodward, *J. Chem. Soc., Dalton Trans.*, 1981, 1134.
8 R. Mason, J. Zubieta, A. T. T. Hseih, J. Knight, and M. J. Mays, *J. Chem. Soc., Chem. Commun.*, 1972, 200.
9 F. A. Cotton and J. M. Troup, *J. Am. Chem. Soc.*, 1974, **96**, 4422.
10 O. Bars and P. Braunstein, *Angew. Chem., Int. Ed. Engl.*, 1982, **21**, 308.
11 A. F. Dyke, S. A. R. Knox, P. J. Naish, and G. E. Taylor, *J. Chem. Soc., Dalton Trans.*, 1982, 1297.
12 B. P. Gracey, S. A. R. Knox, K. A. Macpherson, A. G. Orpen, and S. R. Stobart, *J. Chem. Soc., Dalton Trans.*, 1985, 1935.
13 A. F. Dyke, S. A. R. Knox, M. J. Morris, and P. J. Naish, *J. Chem. Soc., Dalton Trans.*, 1983, 1417.
14 W. A. Herrmann, *Adv. Organomet. Chem.*, 1982, **20**, 159.
15 A. G. Orpen, *J. Chem. Soc., Dalton Trans.*, 1983, 1427.
16 D. L. Davies, S. A. R. Knox, K. A. Mead, M. J. Morris, and P. Woodward, *J. Chem. Soc., Dalton Trans.*, 1984, 2293.
17 S. W. Carr, B. L. Shaw, and M. Thornton-Pett, *J. Chem. Soc., Dalton Trans.*, 1985, 2131.
18 A. Modinos and P. Woodward, *J. Chem. Soc., Dalton Trans.*, 1974, 2065.
19 N. Walker and D. Stuart, *Acta Crystallogr., Sect. A*, 1983, **39**, 158.
20 G. M. Sheldrick, SHELX 76, Program System for *X*-Ray Structure Determination, University of Cambridge, 1976.

Received 14*th May* 1987; *Paper* 7/854